

SOLAR GENERATOR DESIGN USING MATLAB SIMULINK

N.NIKHILA¹, S.PAVANI KUMARI², G.ASHOK³, O.MALINI⁴, K.ANITHA⁵

⁵Guide

Department Of Ece

Tadipatri Engineering College, Tadipatri.

Abstract:

In this study, a solar generator system is modelled and simulated using MATLAB/Simulink. Because of its sustainability and environmental advantages, solar power generation has drawn a lot of attention as interest in renewable energy sources grows. Photovoltaic (PV) panels, a DC-DC converter, and an inverter make up the suggested system, which transforms solar energy into electrical power that may be used. The inverter transforms the DC electricity produced by the PV panels into AC power for use in independent or grid integration applications. A strong foundation for modelling and evaluating such intricate systems is offered by MATLAB/Simulink. The power conversion stages' dynamics, the control algorithms for maximum power point tracking (MPPT), and the electrical properties of the PV panels are all included in the model. Numerous performance metrics, including efficiency, power output, and voltage regulation, are assessed through simulation in a variety of climatic and operational scenarios. The outcomes of the simulation show how efficient and dependable the suggested solar generator system is, offering guidance for improving the design and incorporating it into renewable energy applications.

Keywords: Solar Generator, MATLAB, Simulation, Renewable energy sources, Photovoltaic, PV, PV panels.

INTRODUCTION

The use of renewable power resources for energy era is increasing. But changes are had to meet new technologies with unique criteria for integration with the grid. Wind and photovoltaic renewable electricity technology are present day main technologies, and intermittent power disruptions are a main assignment in each regions. To increase the usage of wind strength and reduce the paintings of backup systems, research is being performed on non-multiplied generation with storage positioned on a separate grid. A DC framework has been proposed to integrate renewable strength and storage. It is commonplace to apply or extra technology for electricity technology on separate systems. Another manner to deal with intermittent wind strength is to mix it with forecasting. This specializes in ways for industries to greater accurately plan how to use products and how to take part in the open market. Wind electricity uncertainty changed into some other studies topic, which led to uncertainty in unit willpower when forecasting wind strength. As proven within the following sections, the potential to alternate the HS output power from non-dispersed generation to semi-dispersed generation is a primary advantage, which permits the device operator to refer to the network programming literature. To reduce the fluctuations in wind electricity generation, the power of power supply relies upon heavily on temporary forecasting and garage ability.

Microgrids (MGs) combine and manipulate disbursed energy assets (DERs) to make certain dependable and strong operation of the local strength machine at some stage in connection to and disconnection from the principle grid. MGs can integrate exclusive varieties of DERs, inclusive of disbursed mills and dispensed garage, digital gadgets, and the load and ability of grid components. For DER interoperability, a power control system (EMS) is required to perform inside the MG [3]. The EMS offers reporting profiles for MG controllers based at the default cause. The use of strength storage structures (ESS) in the MG requires extra technical necessities inside the EMS. In specific, battery-primarily based systems require right kingdom of price (SoC) management to save you speedy degradation. Therefore, the ESS need to additionally be followed through a

battery price controller that forestalls them from being overcharged and absolutely discharged. Meanwhile, the EMS is responsible for proper DER timing, detecting the ideal saved power, and mitigating the pressure because of frequent cycling. This challenge proposes and tests a flexible EMS architecture for battery-based hybrid microgrids to enhance the power reference values provided by means of the DERs working modes. Given a -level system based on ESS fight, the optimization version of the problem involves minimizing the working expenses of the EMS. In this way, the power furnished to the grid is limited, while keeping the secure operating limits of the ESS, which avoids their rapid degradation.

LITERATURE SURVEY

"Analysis, Design and Control of Capacitor Switched Converter Based on Buck and Boost Converter" - Mummati Wirakhari; Vasudha Kupchandani,

This converter has low stage of ripple present day supply regardless of the working mode (step-up, step-down or step-up). First, a likely pulse width modulation (PWM) scheme for the proposed converter is recognized, and then a corresponding performance analysis scheme, consistent-country evaluation and country area version are mounted. Using consistent-nation analysis, the voltage benefit is found out, and the defining equations of the L-C elements are derived based on their ripple values. The nation space models are used to carry out small-sign evaluation and relevant translation operations required in controller layout. The motive of the converter is to control and smoothly switch from step-down mode to step-up mode or vice versa, but the amplitude of the designed voltage/cutting-edge regulator mode is extended.

"A Simple Soft Method to Convert a Buck to a Modified Buck Without Inversion" via Leonardo Gallego; Mihai Cioboda; Daniel J. Pagano; Eugenio Durano; John E. Fletcher,

A new useless-field correction technique is proposed to smooth the transition among running modes, do away with voltage pulses, and enhance trendy characteristics at the same time as maintaining high efficiency. The converter is analyzed with its gate pressure circuit, which is predicated on a power supply with bootstrap capacitors for excessive voltages. The proposed lifeless quarter correction technique is obtained by using the precept of obtaining a sample voltage gain characteristic over the whole converter working variety. The approach is analyzed, implemented and examined on a in particular designed photovoltaic module with a non-inverting greenback-raise converter.

"Grid-balance stepper and invertible glass cladding for maximum electricity generation from two PV arrays under destructive environmental conditions "- Subendu Dutt, Kishore Chatterjee.

Since the inverter can function either in series or in collection relying on the requirement, this mode is significantly decreased to a sub-ordinate form with a minimal variety of series-related PV solar modules. As a result, the strength technology from each subsystem is accelerated whilst faced with special environmental situations. The inverter topology configuration and its manipulate schemes are designed in such a manner that there may be no high-frequency component inside the not unusual-mode voltage, accordingly restricting the amount of current leakage associated with the PV array inside a certain variety. In addition, high working performance is done over the whole operating range. A thorough evaluation of the gadget changed into completed, which brought about a mathematical model of its evolution.

"A Method for Adaptive Vibration Suppression Control in Grid-Connected Photovoltaic Array Inverters" - Hongxu Guo; Matthew Armstrong; Bashar Zahavi

In this examine, an adaptive control set of rules is proposed for grid-connected inverters to suppress resonance situations caused via modifications inside the induction phase because of dynamic modifications inside the operational conditions of the distribution grid. The causes of translation among grid-connected inverters and the distribution grid are mentioned, and the layout of an active bandpass filter out to seize the translation is described. In a proportional-imperative controller, the proportional benefit is adjusted adaptively in real time to make amends for adjustments in network impedance and suppress resonant excitations, whilst preserving high-order low harmonic performance in comparison to the fixed advantage controller mode, specifically for systems with huge network inductance values.

"Phase Synchronization of Photovoltaic Systems with Power Quality Disturbances Using Lossless Kalman Filtering" - Sven Sudarshan; Pidiyadhar Subhuti In this paper, a brand new section synchronization manipulate scheme is proposed for a single-phase PV system with three grid-related phases, which implements a percolation Kalman filtering (UKF) algorithm to compress the fundamental components of the PCC voltage and load modern. The DC capacitance voltage and PCC voltage are controlled via a proportional-critical (PI) controller. The UKF effectively extracts the essential components of the PCC voltage and load modern-day. Simulation and real-global research display that the proposed UKF-PI manage scheme can successfully extract maximum power from the PV machine and reduce the entire harmonic distortion (THD) of the application section present day, thereby decreasing the harmonic load modern. The THD is inside the limits encouraged by way of IEEE 519. The tracking of the meant objective is tested below the sag and upward thrust-go with the flow goal lines. The acquired outcomes show that the network synchronization is effective beneath electricity satisfactory disturbances, along with the community present day is sinusoidal and the PCC voltage is managed by way of imparting suitable reactive electricity.

"Efficient wind-photovoltaic hybrid power era device using brushless twin-induction permanent magnet motor", C. Liu, K.D. Chau, X. Zhang.

In this paper, the performance of AC strength deliver from PMBLDC machine is high. Moreover, the air loss could be very low due to the nature of permanent magnet. The hybrid strength is supplied to DC/DC converter and the voltage is furnished to the burden. The voltage from the hybrid device remains almost steady. Due to the everlasting magnet, the output of PMBLDC isn't sinusoidal. This calls for a nit sensor. Power first-class problems are not explicitly addressed on this paper. A step-down converter is used, so the ripple and THD may also be excessive.

"Automatic Wind Power System Based on Permanent Magnet Synchronous Generator" - C.N. Bende, S. Mishra, Shiv Ganesh Malla.

In this paper, the PMSG presents a constant voltage to the load thru three out of control rectification ranges. This concept does not require a further DC/DC step-down converter. Since this load does no longer require reimbursement, this load is a separate load. This topology best consists of wind generation, which requires an additional capacitor financial institution for strength garage. The power pleasant is not met with the aid of the troubles, so the performance ratio is low. Only the automated technique is mentioned.

"Reactive energy reimbursement and optimization approach for grid-interactive cascaded photovoltaic systems" Liming Liu; Hui Li; Yaosuo Chu; Wenxin Liu.

This paper investigates the effect of reactive power compensation and optimization on system stability and energy satisfactory, and proposes an integrated energetic and reactive electricity distribution to relieve this problem. First, the vector technique of growing the strength distribution policy is explained. Therefore, the relationship among electricity and voltage is developed via the amplitude of the running device. Then, an most useful reactive electricity manage algorithm (RPCA) is proposed to enhance the stableness and reliability of the operating device and facilitate the simultaneous MPPT implementation for every converter module. In addition, an included control gadget with RPCA is developed to permit green electricity distribution and dynamic voltage manage. Results from simulations and experiments are provided to illustrate the effectiveness of the proposed method for reactive strength regeneration in cascade-interconnected photovoltaic systems.

"Simple Technique Reducing Leakage Current for H-Bridge Converter in Transformerless Photovoltaic Generation", Radoslaw Kotet.

Due to their structural configuration, photovoltaic (PV) modules display parasitic capacitance, which facilitates a pathway for high-frequency current during zero-state switching of the converter in transformerless systems. Both objectives of this study are achieved by utilizing a suitable hybrid modulation that minimizes switching losses. In this paper, a separate boost factor is also smaller while a single-order filter is employed. This control technique does not sustain the power compensation.

“Flexible Microgrid Power Quality Enhancement Using Adaptive Hybrid Voltage and Current Controller”, Jinwei He, YunWeiLi, Frede Blaabjerg.

To achieve better harmonic compensation performance using distributed generation (DG) unit power electronics interfaces, an adaptive hybrid voltage and current controlled method (HCM) is introduced in this paper. It demonstrates that the suggested adaptive HCM can diminish the quantity of low-pass/bandpass filters in the DG unit digital controller. Furthermore, phase-locked loops are unnecessary since the microgrid frequency deviation can be automatically detected by the power control loop.

EXISTING SYSTEM

In order to satisfy load requirements, the PV system is programmed to operate under maximum power point tracking (MPPT) when energy generation is low and off-MPPT when energy is in excess. A disturbance compensator is added to the feedback control law that governs the wind energy conversion system (WECS) in order to reject unknown turbine torque and track speed. To run the microgrid as an autonomous system, an energy management algorithm is created that takes into account the battery's condition, the load power requirement, and the power available from renewable sources. Lastly, to guarantee effective power transfer to the load, the voltage at the load side is controlled. A lead acid battery and a bidirectional DC-DC buck-boost converter coupled at the microgrid's DC-link make up the energy storage system (ESS). This converter's job is to keep the DC-link voltage steady even when the load and sources' power fluctuate. The ESS uses a PI control cascade approach to regulate the DC-link voltage.

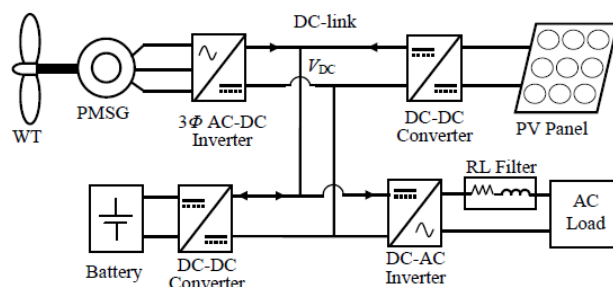


Figure 1: Existing System block diagram

A cascade structure is used in the generator side converter control system to operate at maximum power extraction. To supply the switching pulses for the AC-DC inverter, it has an inner loop current control and an outer loop speed controller. The hybrid isolated micro grid’s converter control is coordinated by the energy management system (EMS). The previous sections presented the control algorithms for those converters. The wind turbine generators AC-DC converter is controlled to regulate rotational speed in order to achieve wind energy MPPT, the PV system's DC-DC converter can operate in either MPPT or off-MPPT modes depending on the system power balance and energy constraints, and the battery's DC-DC converter can operate in either charging or discharging mode depending on the system power balance in order to maintain a constant DC-link voltage.

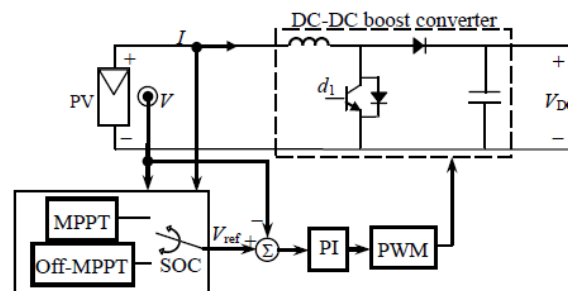


Figure 2: Existing System Circuit diagram

PROPOSED SYSTEM

- NODE MCU microcontrollers are used as the transmission medium in the suggested system.
- Furthermore, this microcontroller communicates faster and produces less noise than an Arduino.

Advantages

- The Node MCU has an advantage over the Arduino in that it has more processors and memory than the Arduino Uno, allowing it to handle larger systems and more complicated devices. Furthermore, the Node MCU has access to two hardware UARTs (UART0 and UART1) with a bit rate of 115,200 and a maximum sharing capacity of 4.5 Mbps.
- It performs better than an Arduino.

BLOCK DIAGRAM

Figure 4.4 displays the block diagram for the suggested smart DC Micro-Grid. The main ac grid, wind, and solar PV are the sources. In addition to the sources, the primary DC bus is interfaced with a battery storage system. DC-DC converters are used to interface all sources to the DC link. A bidirectional buck-boost converter connects the battery storage system. The load side converters drive the loads, as the block diagram illustrates. It is considered that all loads, including fans, lighting, and lab test benches for students' experiments, are priority loads. The proper control modes are used once the power management unit determines the overall amount of power generated and consumed. The findings and discussion section contains a tabulation of the system specifications.

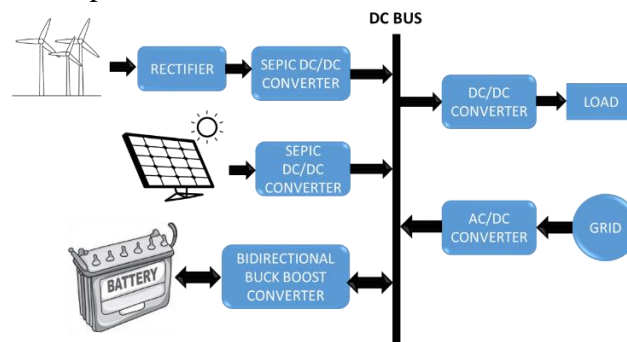


Figure 4: Proposed hybrid power management system

Figure 1 shows a DC micro grid. Low-level control will be provided by the suggested fractional order controllers. The energy management unit oversees the high level control by keeping an eye on power use and generation and producing relevant references for the low level control. The following are the main contributions of this research project.

PV AND WIND ENERGY CONVERTER

Solar and wind energy are both extracted using SEPIC converters. With an input stage akin to a simple boost converter and an output stage akin to a basic buck-boost converter, a SEPIC is a cascaded boost/buck-boost converter. All things considered, a SEPIC function is comparable to a buck-boost converter, but it has the advantages of isolation between the input and output, a true shutdown mode (the converter's output voltage drops to 0V when switch S is turned off), and an output voltage polarity that is not inverted with respect to its input voltage.

An undesirable current cannot flow from the input to the output due to capacitive isolation. The output voltage of the SEPIC is controlled by the duty cycle of switch S. The switch S is usually an electrically controlled switch, like an insulated-gate bipolar transistor (IGBT), power bipolar junction transistor (BJT), or power metal oxide semiconductor field effect transistor (MOSFET). A pulse-frequency modulation (PFM) or pulse-width modulation (PWM) controller regulates its switching operations. A PWM controller changes the duty cycle of switch S while maintaining a constant switching frequency, whereas a PFM controller changes the switching frequency of switch S while maintaining a constant duty cycle.

BASIC SEPIC OPERATION

Through energy exchange between its coupling capacitor and switching inductors (Cin, L1, and L2), the basic SEPIC converts DC-DC voltage. The switch regulates how much energy is exchanged between the inductors

and capacitor. This SEPIC design must function in continuous conduction mode (CCM) in order to maximize energy exchange efficiency and overall converter efficiency.

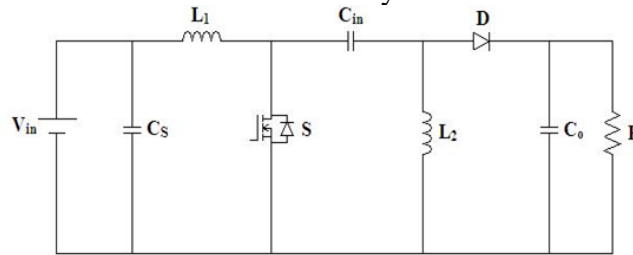


Figure 5: SEPIC converter

Continuous Conduction Mode

The inductor current will never stop flowing when operating in the continuous conduction mode. This implies that in order to operate the SEPIC in CCM, the currents via L_1 and L_2 must never drop below 0A, or let them discharge entirely. The average voltage across C_{in} will match V_{in} 's when the SEPI reaches steady-state operation. In addition, the steady-state average current through C_{in} is 0A. L_2 is the only source of current flowing to the output load when this steady-state occurrence takes place. As a result, L_2 's average current is independent of V_{in} and equals the output load.

When switch is close

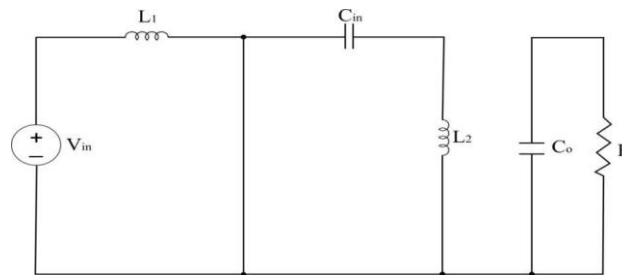


Figure 6: Switch on condition

When switch S conducts, the SEPIC operates as seen in Figure 6. Since it is assumed that filter capacitors C_s and C_o remain in a steady-state, no current passes through them until they discharge. Additionally, it is believed that C_s and C_o have capacitances that are sufficiently big to almost eliminate the ripple voltages in the SEPIC's input and output.

The current through L_1 increases in a positive direction and the current through L_2 increases in a negative direction when switch S conducts during the first half-switching cycle. Thus, L_2 discharges (functioning as a source) through C_{in} , whereas L_1 charges via V_{in} . S stays closed for a brief moment, during which the instantaneous voltage across C_{in} is equal to V_{in} . Thus, the magnitudes of V_{L1} and V_{L2} are about equal to V_{in} .

Since L_2 is discharging, the only difference between the two voltages is that V_{L2} 's polarity is reversed, or negative. In order to store energy in L_2 , C_{in} discharges and supplies current to L_2 . This allows L_2 to supply current to the output load when switch S stops conducting during the subsequent half-switching cycle. Diode D is reverse-biased, meaning it does not conduct for this full half-switching cycle. When switch S is conducting, C_o discharges and is the only part that keeps the output load current constant. Switch S shuts off during the second half-switching cycle.

When switch is opened

When the switch is opened, Figure 3.6 illustrates how the SEPIC operates. Switch S shuts off after one half-switching cycle. Through L_1 and C_{in} , the input current has a new path. Inductor currents can not change instantly because current cannot flow through an inductor in an instant. Capacitor current C_{in} is therefore

equal to $L1$ current. While $L2$ is still discharging, it discharges into C_o throughout this half-switching cycle, activating D , or forward biasing, and providing current to the output load.

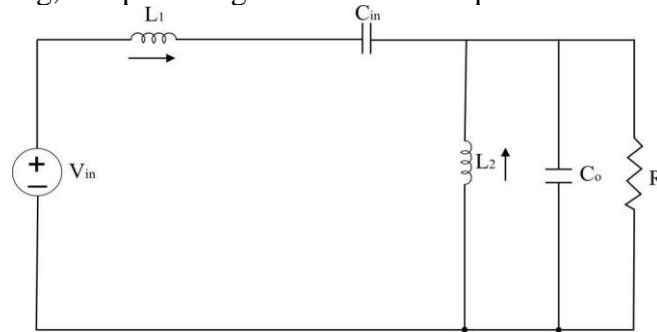


Figure 7: Switch off condition

$L2$ current, however, adds to the input current that already flows to the output load due to its direction. Consequently, both $L1$ and $L2$ provide current to the output load when S is not conducting. V_{in} and $L1$ charge C_{in} , which discharged when switch S conducted during the half-switching cycle. $L2$ then discharges to the output load until switch S conducts once more at the start of the subsequent half-switching cycle, when C_{in} provides current to charge $L2$.

Discontinuous Conduction Mode

The inductor current drops to zero when operating in the discontinuous conduction mode. If the currents flowing through $L1$ and $L2$ stay at $0A$ for any length of time in comparison to the switch flipping duration, the discontinuous conduction mode takes place. Higher efficiency is achieved at lower current loads when a SEPIC is operated in DCM; nevertheless, greater current loads are necessary. Consequently, higher total converter efficiency should result from operating in CCM.

DESIGN OF SEPIC CONVERTER

The right component values must be chosen in order to design the SEPIC for correct operation under the suggested specifications.

The SEPIC is made up of the capacitor C_{in} , diode D , switching transistor S , and inductors $L1$ and $L2$. To reduce input and output voltage ripple, the capacitance of the input and output filter capacitors, C_s and C_o , must also be sufficiently big. Due to a pulsating diode (D) connected to its output, the SEPIC topology has a significant drawback in that its output voltage ripple is naturally high. As previously stated, a pulsing current is delivered to the converter's output because D conducts when switch S is off and does not conduct when switch S is on. Therefore, in order to properly suppress any output voltage ripple caused by diode pulsing current, C_o must have a large capacitance.

Because MOSFETs have a higher input impedance and a lower voltage drop across their principal current route than BJTs, they are better for switches. Additionally, a BJT requires additional resistors to bias it because, in contrast to MOSFETs, which control switching by voltage differences, BJT switching is controlled by current differences.

The following formulas were utilized in the SEPIC converter's design:

INDUCTOR CURRENT

$$I_L = \frac{I_{OUT} \times V_0 \times 40\%}{V_{IN(min)}} \tag{4.3}$$

INDUCTOR L₁ & L₂

$$L_1 = L_2 = \frac{V_{IN(min)} \times D_{max}}{\Delta I_L \times F_{SW}} \tag{4.4}$$

OUTPUT RIPPLE VOLTAGE

$$\Delta V_{CIN} = \frac{I_{OUT(max)}}{C_{IN} \times F_{SW}} \times \frac{V_{OUT}}{V_{IN} + V_{OUT} + V_D} \tag{4.5}$$

OUTPUT CAPACITOR

$$C_{OUT} = \frac{I_{OUT} \times D_{max}}{V_{RIP} \times 0.5 \times F_{SW}} \tag{4.6}$$

The design parameters that aid in controlling the brushless DC motor's commutation circuit input are computed using the aforementioned equations.

PI CONTROLLER

The PI Controller block diagram is displayed in the figure below. The voltage of the DC side capacitor is measured and contrasted with a reference voltage. The PI Controller uses this error, $e = V_{dc, ref} - V_{dc}$, as an input. A Low Pass Filter (LPF) based on the Butterworth design processes the error signal.



Figure 8: PI Controller

With a cutoff frequency of 50 Hz, the LPF filter can suppress higher order components and only permit fundamental ones. $H(s) = K_p + K_i/s$ is the representation of the PI Controller's transfer function (4.7).

Where K_i is the integration constant that controls the DC-side voltage control's settling time and K_p is the proportional constant that controls its dynamic response. The DC-side voltage's study state error is being eliminated by the proportional integral controller.

BATTERY STORAGE CONVERTER

Figure 4 displays the battery storage system block diagram. The battery storage system is integrated with the microgrid's primary DC bus via a buck boost converter. Battery storage systems can operate in either charging or discharging mode, depending on the state of charge (SOC), source side power availability, and load side power demand. The converter operates in buck mode when charging since power is transmitted from the main bus to the batteries. The battery converter is in boost mode when power is returned to the microgrid. The following is the derivation of the battery converter system's mathematical model.

1. Boost mode: When the energy management system is in boost mode, the reference battery current is positive. Thus, the following is a model of the boost mode:

$$\frac{dI_b}{dt} = \frac{V_b}{L_b} - (1 - U_{Q1}) \frac{V_{dc}}{L_b} + D_7$$

$$\frac{dV_{dc}}{dt} = (1 - U_{Q1}) \frac{I_b}{C_{dc}} - \frac{I_{ob}}{C_{dc}} + D_8$$

Where U_{Q1} is the control signal, I_b is the battery current, and V_b is the battery voltage. The power stage parameters' uncertainty dynamics are denoted by the words D_7 and D_8 .

2. **Buck mode:** In buck mode, the reference battery current generated by the energy management system is negative. So the buck mode is modeled as follows:

$$\frac{dI_b}{dt} = \frac{V_b}{L_b} - U_{Q2} \frac{V_{dc}}{L_b} + D_7$$

$$\frac{dV_{dc}}{dt} = U_{Q2} \frac{I_b}{C_{dc}} - \frac{I_{ob}}{C_{dc}} + D_8$$

Where UQ2 is the buck mode control signal. The generalized model representing the buck and boost mode is expressed as follows:

$$\frac{dI_b}{dt} = \frac{V_b}{L_b} - U_4 \frac{V_{dc}}{L_b} + D_7$$

$$\frac{dV_{dc}}{dt} = U_4 \frac{I_b}{C_{dc}} - \frac{I_{ob}}{C_{dc}} + D_8$$

The boost mode control UQ1 is active when sw = 1, and the buck mode controller UQ2 is active when sw = 0.

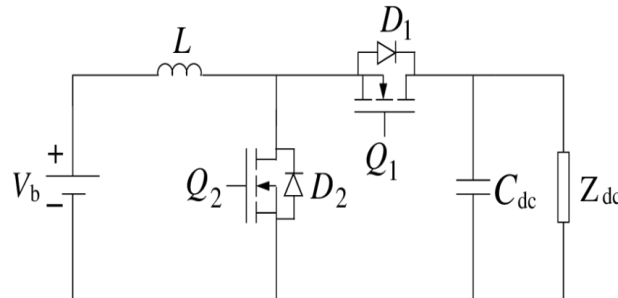


Figure 9: Battery Storage Converter Module

ENERGY MANAGEMENT UNIT

The unit calculates the available input power from wind and photovoltaic sources. Similar to this, the load side's power consumption is measured as well. The energy management algorithm is then created using a power balance equation, as illustrated in Figure 6. Priority is given to using input sources like wind and photovoltaic systems to supply the loads. The energy storage system is charged when there is an abundance of power coming from input sources. Under typical operating circumstances, no electricity is taken from the AC grid. Power from the AC grid is used to power the loads in situations where the electricity from the PV, wind, and battery storage systems is insufficient.

CONCLUSION

This paper proposes a novel approach to maximize the usage of solar and wind power generation on self-consumption infrastructures. Depending on the measured source and load powers, an energy management unit is used to activate the proper mode of the controllers. In order to make the micro grid as cost-effective as possible with necessary loads and no load shedding plan, the energy management unit gives priority to renewable energy sources (wind and photovoltaic). The energy management algorithm is validated and the suggested controller is successfully put into use. Additionally, for uncertain system characteristics, the performance of the suggested fractional order controller is contrasted with that of the integer order controller (Appendix II). The performance of the suggested controller was better than that of the integer control method.

REFERENCES:

[1] Mummadi Veerachary; Vasudha Khubchandani, "Analysis, Design, and Control of Switching Capacitor Based Buck–Boost Converter", IEEE Transactions on Industry Applications, vol. 55, no. 3, pp. 2845 – 2857,2019.

- [2] Leonardo Callegaro ; Mihai Ciobotaru ; Daniel J. Pagano ; Eugenio Turano ; John E. Fletcher, “A Simple Smooth Transition Technique for the No inverting Buck–Boost Converter”, IEEE Transactions on Power Electronics, vol. 33, no. 6, pp. 4906 – 4915, 2018.
- [3] Subhendu Dutta ; Kishore Chatterjee , A Buck and Boost Based Grid Connected PV Inverter Maximizing Power Yield From Two PV Arrays in Mismatched Environmental Conditions, IEEE Transactions on Industrial Electronics, Volume: 65 , Issue: 7 , July 2018.
- [4] Hongsoo Goh ; Matthew Armstrong ; Bashar Zahawi, ”Adaptive control technique for suppression of resonance in grid-connected PV inverters”, IET Power Electronics, Volume: 12 , Issue: 6 , 2019
- [5] Sudarshan Swain; Bidyadhar Subudhi, “Grid Synchronization of a PV System With Power Quality Disturbances Using Unscented Kalman Filtering”, IEEE Transactions on Sustainable Energy, Volume: 10 , Issue: 3 , July 2019.
- [6] Chunhua Liu ; K. T. Chau ; Xiaodong Zhang, An Efficient Wind–Photovoltaic Hybrid Generation System Using Doubly Excited Permanent-Magnet Brushless Machine, IEEE Transactions on Industrial Electronics, Volume: 57 , Issue: 3 , March 2010.
- [7] C. N. Bhende ; S. Mishra ; Siva Ganesh Malla, Permanent Magnet Synchronous Generator-Based Standalone Wind Energy Supply System, IEEE Transactions on Sustainable Energy, Volume: 2 , Issue: 4 , Oct. 2011.
- [8] Liming Liu; Hui Li ; Yaosuo Xue ; Wenxin Liu, Reactive Power Compensation and Optimization Strategy for Grid-Interactive Cascaded Photovoltaic Systems, IEEE Transactions on Power Electronics, Volume: 30, Issue: 1, Jan. 2015.
- [9] Kot, Radoslaw; Stynski, Sebastian; Stepień, Krzysztof; Zaleski, Jaroslaw ;Malinowski, Mariusz, “Simple Technique Reducing Leakage Current for H-Bridge Converter in Transformerless Photovoltaic Generation”, Journal of Power Electronics, Volume 16, Issue 1, pp.153-162, 2016.
- [10] Jinwei He, Yun Wei Li, Blaabjerg, F., “Flexible Microgrid Power Quality Enhancement Using Adaptive Hybrid Voltage and Current Controller”, IEEE Trans. Ind. Electron., vol.61, no.6, pp.2784-2794, June 2014.